Flash Flood–Producing Storm Properties in a Small Urban Watershed

BRIANNE K. SMITH,[a] JAMES SMITH, AND MARY LYNN BAECK

Department of Civil and Environmental Engineering, Princeton University, Princeton, New Jersey

(Manuscript received 15 March 2016, in final form 24 June 2016)

ABSTRACT

The structure and evolution of flash flood–producing storms over a small urban watershed in the mid-Atlantic United States with a prototypical flash flood response is examined. Lagrangian storm properties are investigated through analyses of the 32 storms that produced the largest peak discharges in Moores Run between January 2000 and May 2014. The Thunderstorm Identification, Tracking, Analysis, and Nowcasting (TITAN) algorithm is used to track storm characteristics over their life cycle with a focus on storm size, movement, intensity, and location. First, the 13 June 2003 and 1 June 2006 storms, which produced the two largest peak discharges for the study period, are analyzed. Heavy rainfall for the 13 June 2003 and 1 June 2006 storms were caused by a collapsing thunderstorm cell and a slow-moving, low-echo centroid storm. Analyses of the 32 storms show that collapsing storm cells play an important role in peak rainfall rate production and flash flooding. Storm motion is predominantly southwest-to-northeast, and approximately half of the storms exhibited some linear organization. Mean storm total rainfall for the 32 storms displayed an asymmetric distribution around Moores Run, with sharply decreasing gradients southwest of the watershed (upwind and into the city) and increased rainfall to the northeast (downwind and away from the city). Results indicate urban modification of rainfall in flash flood–producing storms. There was no evidence that the storms split around Baltimore. Flood-producing rainfall was highly concentrated in time; on average, approximately 21% of the storm total rainfall fell within 15 min.

1. Introduction

Flash flooding in urban watersheds causes fatalities (Mooney 1983; Ashley and Ashley 2008), damages (Ogden et al. 2000), and degradation of stream channel health (Booth 1990; Paul and Meyer 2001). These impacts can be mitigated through better flash flood forecasting and urban storm water infrastructure design, which is often based on design storm calculations. In this study, we seek to characterize storms that cause flash flooding in a prototypical flash flood–prone urban watershed on the U.S. East Coast.

Small urbanized watersheds flood in response to short-term, high-intensity rainfall (Morin et al. 2001; Berne et al. 2004; Wright et al. 2012; Smith et al. 2013). Thunderstorm systems are responsible for more than half of flash floods in U.S. urban watersheds east of the Rocky Mountains (Smith and Smith 2015). Previous studies examined flash flood–producing storms from a large-scale perspective. Maddox et al. (1979) investigated the synoptic- and meso-α-scale conditions leading to flash flood–producing storms across the contiguous United States. Therein they identified common features including association with convective storms, repeated formation of convective cells in the same area, and storm occurrence during nighttime hours. Characteristics identified by Maddox et al. (1979) were investigated on a storm basis for many flood events in the central and eastern United States (Pontrelli et al. 1999; Schumacher and Johnson 2008; Schwartz et al. 1990; Elsner et al. 1989). The organization of flash flood–producing storms has been found to vary nationally, with mesoscale convective systems producing up to 65% of heavy precipitation events east of the Rocky Mountains (Schumacher and Johnson 2005). In the Northeast, scattered, cellular modes of convection are more common (Jessup and Colucci 2012).

[a] Current affiliation: Department of Earth and Environmental Sciences, Brooklyn College of the City University of New York, Brooklyn, New York.

Corresponding author address: Brianne K. Smith, Department of Earth and Environmental Sciences, Brooklyn College of the City University of New York, 2900 Bedford Ave., Brooklyn, NY 11210. E-mail: brianne.smith43@brooklyn.cuny.edu

DOI: 10.1175/JHM-D-16-0070.1

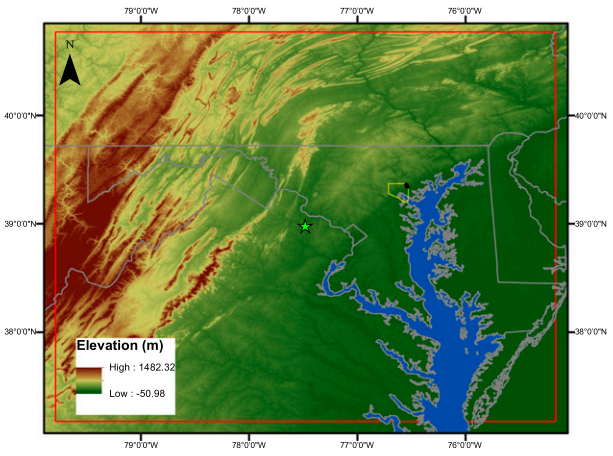

FIG. 1. Study area map with elevation. Moores Run is represented in black, and Baltimore is outlined in yellow. The KLWX radar at Sterling, VA, is represented by a green star. The red box outlines the extent used for TITAN analyses. Chesapeake Bay is colored blue for clarity.

We investigate flash flood–producing storms in a prototypical flashy urban watershed in the mid-Atlantic United States. Moores Run is a small (9.1 km^2) urban watershed in Baltimore, Maryland, that has a characteristic flood response time of approximately 15 min (Smith et al. 2005, 2013). Moores Run displays the quintessential flash flood response for a small urban watershed by rapidly concentrating runoff in large storm drains (Smith et al. 2005).

A Lagrangian perspective is used to examine storm structure and evolution as storms pass over Moores Run. This Lagrangian storm-tracking perspective has been used for a number of studies of heavy precipitation (Tapia et al. 1998; Niyogi et al. 2011; Thorndahl et al. 2014), particularly to objectively examine large storm samples (Javier et al. 2007; Peleg and Morin 2012; Yeung et al. 2015). Automated storm tracking can result in some errors in identifying storm cell evolution and splitting/merging (e.g., Lakshmanan and Smith 2010); however, it also allows for objectively processing large storm samples in ways that would not be possible otherwise. The Thunderstorm Identification, Tracking, Analysis, and Nowcasting (TITAN) algorithms are used to follow the flash flood–producing storms in time using 3D volume scan reflectivity (Dixon and Wiener 1993). TITAN has been used to examine Lagrangian storm properties in the New York–New Jersey urban environment (Yeung et al. 2015).

Previous studies have examined aspects of the rainfall climatology and storm evolution for the Baltimore metropolitan region. Ntelekos et al. (2007) examined the life cycle of flash flood–producing thunderstorms and identified pronounced seasonal and diurnal cycles to flash flood–producing thunderstorm occurrence, with peaks in the warm season and evening (2100–2200 UTC). Heavy rainfall for the 13 June 2003 flash flood event in Moores Run was found to be caused by collapse of a convective storm cell over the Moores Run watershed (Smith et al. 2005).

Other studies have focused on urban modification of rainfall in the Baltimore region. Urban areas can cause downwind rainfall maxima, as a result of urban heat island effects, increased surface roughness, and urban aerosols (Shepherd 2005). A 10-yr, bias-corrected radar rainfall dataset was developed using the Hydro-NEXRAD system and a collection of rain gauges to investigate rainfall climatology in the Baltimore area (Smith et al. 2012). Minima in warm season rainfall were observed in the Maryland Piedmont region and west of Baltimore. Pronounced maxima in warm season rainfall were observed northeast of Baltimore. Atmospheric modeling studies have interpreted the regional climatology of extreme rainfall and urban modification of rainfall (Ntelekos et al. 2008; Li et al. 2013; Ryu et al. 2016). Moores Run is located in the northeast (downwind) corner of Baltimore and experiences slightly higher short-term rainfall rates than other similarly sized watersheds in the region, likely as a result of its location (Smith et al. 2013). Some studies outside of the Baltimore region have suggested that thunderstorms may also bifurcate around cities (Bornstein and Lin 2000; Niyogi et al. 2011).

TABLE 1. TITAN parameters.

Parameter	Definition	Track type[a]
Total area	Area of entire storm	Complex track
Speed	Storm speed	Averaged value of all simple tracks in complex track
Direction	Direction of storm cell motion	Representative simple track
Max reflectivity	Largest reflectivity value in storm cell	Extended simple track
Eco top	Tallest height of 45 dBZ threshold	Extended simple track
Max reflectivity height	Height of max reflectivity value	Extended simple track

[a] Representative simple track is the track with the largest area at each time step, and extended simple track is the dominant simple track at each time that extends from the flood-producing simple track.

TABLE 2. Top 32 discharge peaks in Moores Run from January 2000 to May 2014. Asterisks indicate where values are estimated.

Peak rank	Peak time (EST)	Date	Peak discharge ($m^3 s^{-1}$)	Max 15-min rain rate ($mm h^{-1}$)	Storm total rainfall (mm)
1	1924*	13 Jun 2003	124.0	131	47
2	1918	1 Jun 2006	114.6	66	59
3	2103	10 Jun 2013	103.4	104	106
4	2218	12 Aug 2010	95.1	78	154
5	1621	16 Nov 2006	83.0	48	66
6	1310	30 Sep 2010	69.9	39	144
7	0144*	3 Aug 2002	69.4	100	72
8	2238	2 Jun 2006	68.2	38	48
9	0442	23 Sep 2003	66.9	36	60
10	2353	7 Sep 2011	66.8	67	57
11	2255	29 Jun 2012	61.7	113	59
12	0959	14 Aug 2011	59.7	52	39
13	2323	5 Jul 2006	58.9	93	147
14	1545	13 Jun 2013	56.4	47	30
15	2106	6 Jul 2003	56.3	62	38
16	1454	30 Apr 2014	53.8	44	148
17	1336	21 Aug 2011	53.0	31	29
18	1433	23 Sep 2011	53.0	54	132
19	1531	17 May 2004	52.8	32	16
20	1342	13 Aug 2011	52.7	51	39
21	1251	7 Sep 2011	52.4	44	115
22	2102	1 Jul 2009	50.2	45	35
23	2044	27 Jul 2004	49.7	80	106
24	2036	23 Jul 2008	47.8	66	47
25	1509	19 Jul 2011	46.2	35	21
26	1447	27 Sep 2008	45.6	51	97
27	0152	7 Jul 2008	44.6	89	55
28	2149	27 Jun 2006	44.2	37	157
29	1646	12 Jun 2003	42.2	75	64
30	2121	16 Jul 2005	40.8	30	43
31	1900	25 May 2004	40.5	39	19
32	1701	22 Jul 2006	40.2	54	24

Our analyses of flash flood–producing storm properties in Moores Run are designed to provide a better understanding of rainfall processes that cause flash flooding in urban areas. We use a collection of 32 storm events to determine the characteristic properties of storm structure and evolution for flash floods in small urban watersheds in the mid-Atlantic United States.

2. Study area, data, and methodology

Moores Run is a 9.1 km^2 urban watershed in Baltimore, Maryland (94% in the city of Baltimore and 6% in Baltimore County; see Fig. 1). Runoff in Moores Run is rapidly concentrated in storm drains, resulting in response times between the rainfall volume centroid and peak discharge as short as 15 min (Smith et al. 2005). Moores Run floods in response to intense short-term (15–60 min) rain rates (Smith et al. 2013). We focus on Moores Run because of its rapid hydrologic response. Moores Run is one of the flashiest watersheds in the country (Smith and Smith 2015) and is chosen for its prototypical urban flash flooding. Much work has been done to investigate the hydrologic properties of Moores Run (Smith et al. 2005; Nelson et al. 2006; Meierdiercks et al. 2010; Bhaskar and Welty 2012; Smith et al. 2013; Schwartz and Smith 2014) as well as the rainfall climatology and storm evolution for the area (Ntelekos et al. 2007, 2008; Smith et al. 2012, 2013).

This study is based on analyses of the largest 32 discharge peaks in Moores Run from January 2000 through May 2014. Moores Run streamflow data, with a 1-min time resolution, were obtained from the U.S. Geological Survey (USGS) Instantaneous Data Archive (pre-October 2007, http://ida.water.usgs.gov/ida/) and the USGS Instantaneous Values Service (post-October 2007, http://waterservices.usgs.gov/rest/IV-Test-Tool.html). Instantaneous streamflow data were updated using corrected stage–discharge relationships. Discharge peaks were calculated as local maxima in instantaneous streamflow separated by at least 6 h. Missing discharge peaks were supplemented with USGS annual peak data. One discharge peak was excluded because of missing radar rainfall data,

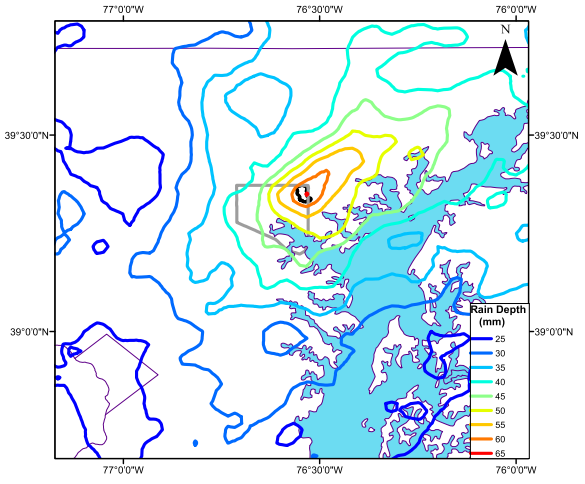

FIG. 2. Storm-averaged rainfall map (contours; mm) for all 32 storm events. Moores Run is outlined in black, Baltimore is outlined in gray, and Chesapeake Bay is colored blue for clarity.

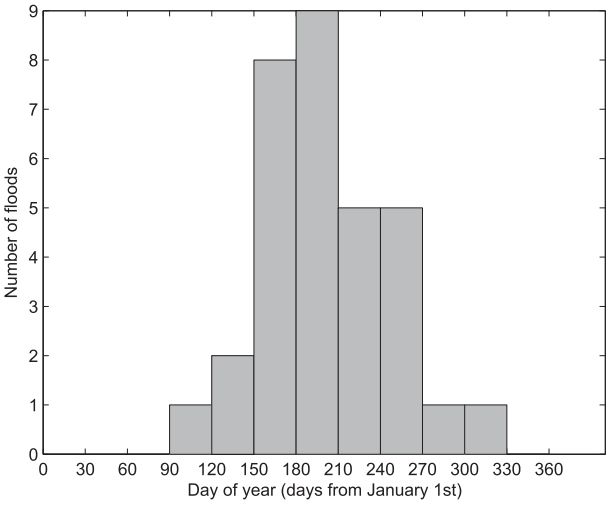

FIG. 3. Histogram of flood peak seasonality.

the 19 July 2012 flood with the sixteenth-largest discharge peak ($55\,m^3\,s^{-1}$).

The Hydro-NEXRAD system (Smith et al. 2012; Krajewski et al. 2011) was used to develop $1\,km^2$ rainfall fields from the Sterling, Virginia, WSR-88D radar reflectivity fields. Radar rainfall fields were bias corrected with rain gauge data. For storms through December 2009, multiplicative bias values were developed through a diverse network of rain gauges (see Smith et al. 2012) and for storms after January 2010, Community Collaborative Rain, Hail, and Snow Network (CoCoRaHS) rain gauges (http://www.cocorahs.org) were used for bias correction (as in Smith et al. 2015). Basin-averaged rain rates at a 15-min time resolution were derived from the bias-corrected radar rainfall fields.

Storm tracking was performed using the TITAN system with 3D radar reflectivity fields (Dixon and Wiener 1993). The TITAN domain is shown in Fig. 1 and covers the range of the KLWX WSR-88D radar in Sterling, Virginia. TITAN identifies storm cells that exceed a specified threshold in reflectivity over a contiguous specified volume threshold. A centroid tracking algorithm (Austin and Bellon 1982) is optimized to track these storm cells between successive radar scans. Storm cells can merge or split in time, creating simple and complex tracks. Simple storm tracks represent storm cells during a period of time during which they do not split or merge with other storm cells. Complex storm tracks represent all storm cells that split or merge with each other at some point in the TITAN domain and specified time period. In this study complex storm tracks may consist of a single simple track or multiple simple tracks. TITAN records a number of storm attributes through time for each simple track, including area, speed, direction, maximum reflectivity, echo-top height, and maximum reflectivity height (Table 1). For this study, storm identification thresholds of 45 dBZ and $50\,km^2$ were set. These thresholds help to identify convective storm elements and exclude stratiform precipitation [for threshold guidelines, see Dixon and Wiener (1993), and for use of other thresholds, see Javier et al. (2007)].

To interpret storm-tracking results, the flood-producing storm cell was identified manually through visual inspection of 3D reflectivity fields with the tracked storm elements. The simple and complex track numbers as well as the time at which the storm cell hit

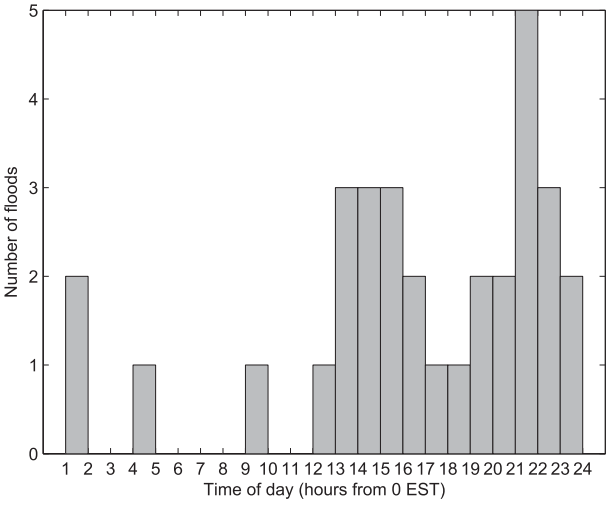

FIG. 4. Histogram of hour of day for flood peak discharge.

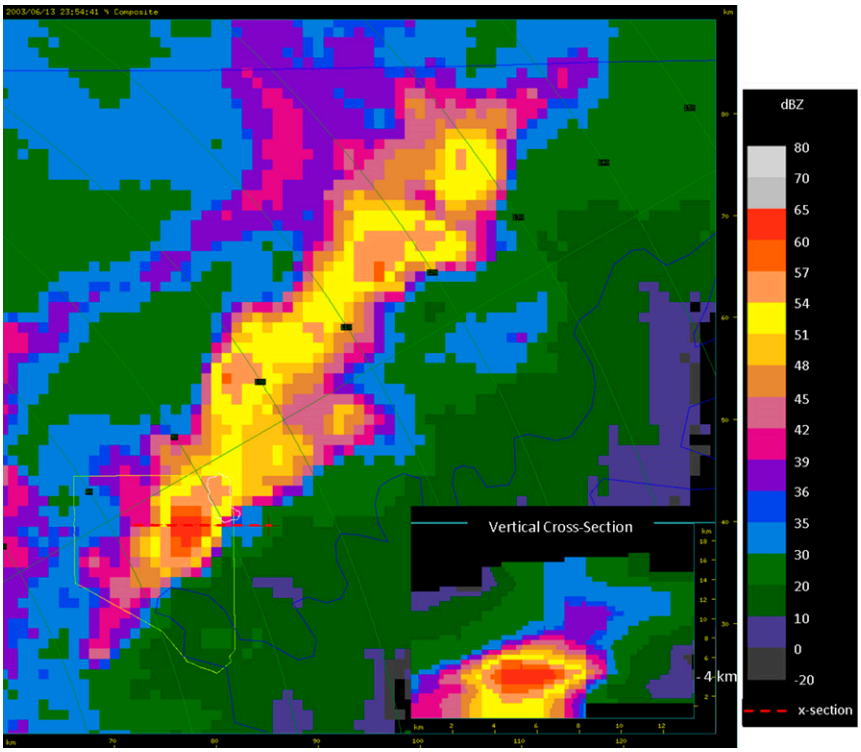

FIG. 5. Radar map and vertical cross section for the 13 Jun 2003 storm at 2354 UTC 13 Jun 2003. Moores Run is in white and Baltimore is outlined in yellow. The red dashed line shows the location of the vertical cross section.

Moores Run were recorded. The storm cell was assumed to hit Moores Run when the boundaries of the storm cell were most directly over the watershed. This generally occurred 15–30 min before the flood peak discharge. For time series analyses, the time the storm cell reaches Moores Run was set as time 0 to allow for comparison of storm evolution across flash flood events. To analyze storm structure and evolution, several approaches were used to compute time series for different storm attributes (Table 1).

3. Results and discussion

a. Storm discharge and rainfall

The 32 storm events with the highest peak discharges from January 2000 to May 2014 have peak discharge values ranging from 40 to 124 $m^3 s^{-1}$ (Table 2). The maximum 15-min rain rate for these storm events ranges from 30 to 131 $mm\,h^{-1}$. Large peak discharge values do not directly correspond to large values of maximum 15-min rain rate. The Pearson correlation coefficient between peak discharge and maximum 15-min rain rate is 0.52.

The map of the storm-averaged rainfall for the 30 storm events shows an asymmetric distribution of rainfall concentrated around the Moores Run watershed (Fig. 2). The spatial concentration of rainfall highlights the localized, intense rainfall that causes flash flooding in Moores Run. A similar analysis of flash flood–producing rainfall in a nonurban Baltimore County watershed exhibits much smoother rainfall contours, suggesting that urban watersheds are particularly prone to flooding from intense, spatially concentrated rainfall (Smith et al. 2013). There are sharp gradients in rainfall around the local maximum in Moores Run, especially to the southwest (upwind and into the city), which exhibits a decrease of approximately 1.8 $mm\,km^{-1}$ between the maximum rainfall contour of 65 mm and the 55-mm contour. Northeast (downwind) of Moores Run, rainfall gradients are approximately 0.6 $mm\,km^{-1}$ for the storm total rainfall between the maximum rainfall contour of 65 mm and the 55-mm contour. The extensive region of elevated rainfall to the northeast of Moores Run and Baltimore corresponds to the observed downwind rainfall maxima in the Baltimore area (Smith et al. 2012). This element of the regional rainfall climatology has been linked to the interacting effects of the urban heat island circulation and the bay breeze circulation (see Ryu et al. 2016).

The average storm total rainfall over Moores Run is 71 mm, while the average maximum 15-min accumulation

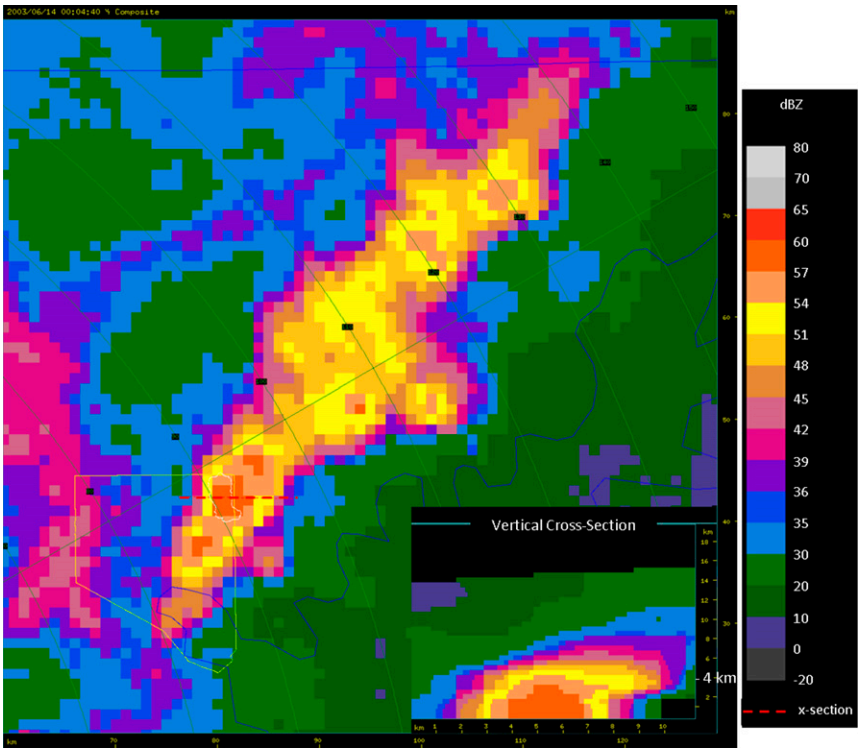

FIG. 6. As in Fig. 5, but for the 13 Jun 2003 storm at 0004 UTC 14 Jun 2003.

is 15 mm, suggesting that 21% of the storm rainfall tends to come in the most intense 15 min of rainfall. On average for the 32 storm events, 21% of the storm total rainfall falls within 15 min, 34% falls within 30 min, and 48% falls within 1 h. The rainfall that causes flash flooding in Moores Run is both spatially and temporally concentrated.

The 32 storm events occur primarily during the warm season. A histogram of storm occurrence throughout the year shows increased occurrence during summer months (Fig. 3), and a probability density function of storm occurrence has a peak around 22 July (the 203rd day of the year). The tendency for warm season thunderstorms to cause flooding in urban areas has been observed in the Baltimore area (Ntelekos et al. 2007; Smith et al. 2013) and nationally (Doswell et al. 1996; Yang et al. 2013). Flood peaks tend to occur in the evening, with a peak in the diurnal probability density function around 2200 eastern standard time (EST; for histogram see Fig. 4). Flood peaks with missing times were assumed to occur 20 min after the storm cell reached Moores Run.

b. *13 June 2003 storm*

The 13 June 2003 and 1 June 2006 storms caused the two largest discharge peaks in Moores Run. These storms are presented as examples of two potential storm patterns that cause flash flooding in the Moores Run watershed. Results obtained from these two storms will be extended to the entire 32-storm sample in later sections.

The 13 June 2003 flood peak is the flood of record in Moores Run. This event was not represented in USGS instantaneous streamflow data because the stream gauge was not operational during the flood. Modeling studies to recreate the storm hydrograph based on radar rainfall fields indicate that the discharge peak occurred at approximately 1924 EST 13 June 2003 (Smith et al. 2005).

The 13 June 2003 storm was a linearly organized multicell thunderstorm (Figs. 5–7). An intense storm cell with reflectivity values of 65 dBZ at 4.5 km height moved through Baltimore toward Moores Run. The storm cell collapsed as it decayed and entered a downdraft-dominated phase over Moores Run. The collapse was observed through a decrease in reflectivity and echo-top height on radar reflectivity scans. This storm cell collapse coincided with maximum rainfall measurements from local rain gauges (Smith et al. 2005). Basin-averaged rainfall for the storm is estimated at 47 mm, which is below average for the 32-storm sample (Table 1). Maximum 15-min rainfall intensity is estimated to be

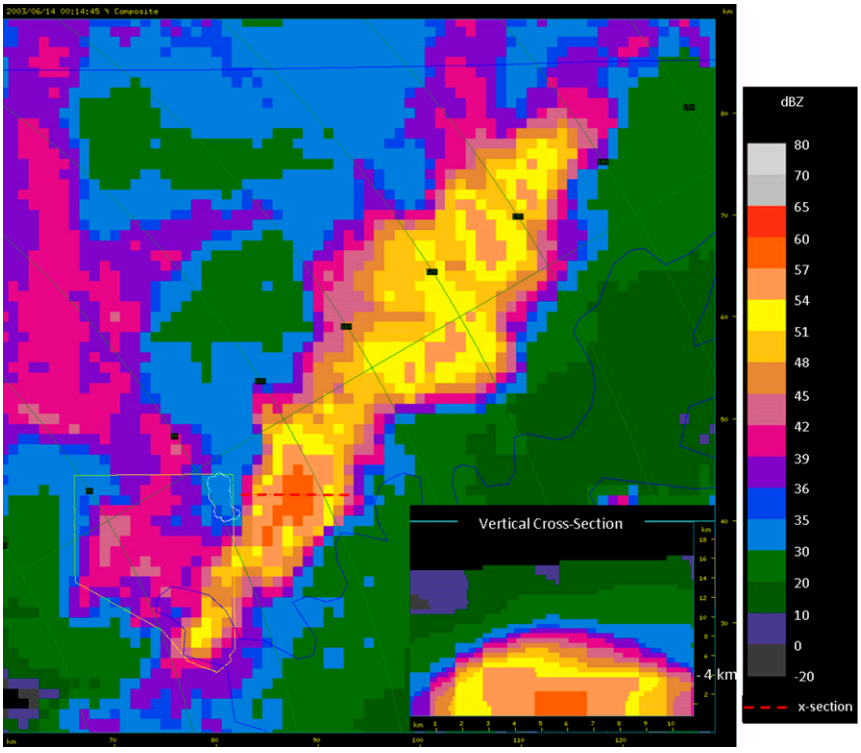

FIG. 7. As in Fig. 5, but for the 13 Jun 2003 storm at 0014 UTC 14 Jun 2003.

131 mm h^{-1}, which is the largest peak rain rate in the 32-storm sample (Table 1). Average basin-averaged rainfall for all 32 events is 71 mm, and the average maximum 15-min rainfall intensity for the 32 events is 60 mm. Flooding for the 13 June 2003 storm was driven by this high 15-min rainfall rate, which resulted from storm cell collapse.

Storm-tracking analyses highlight the changing structure of the storm system that passed over Moores Run. The area is at its maximum (1181 km^2, Fig. 8) as the storm passes over Moores Run (time 0) and decreases

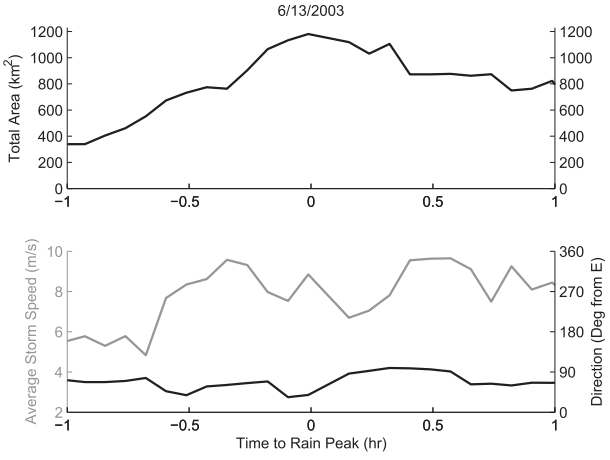

FIG. 8. Storm characteristics time series for the 13 Jun 2003 storm. (top) Total area of the flood-causing complex storm track. (bottom) Average speed of all simple tracks within the flood-causing complex track (gray) and direction of the simple track with the largest area (black; counterclockwise degrees from east). Time 0 represents the time that the flood-producing storm cell was over Moores Run.

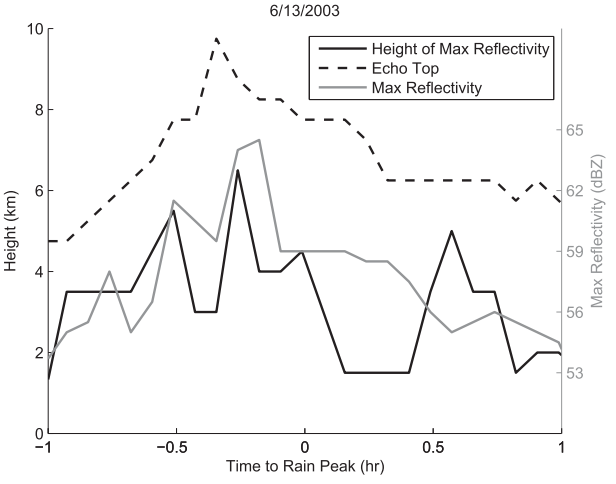

FIG. 9. Storm characteristics time series for the 13 Jun 2003 storm. Max reflectivity, height of max reflectivity, and echo-top height for the extended simple track.

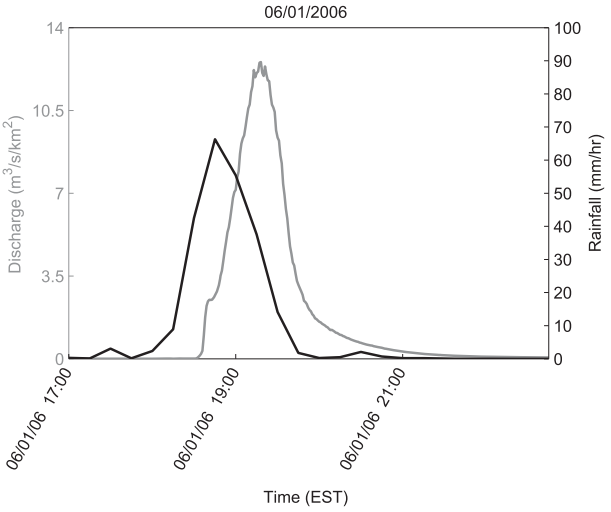

FIG. 10. Plot of hydrograph and rainfall for 1 Jun 2006 storm.

rapidly after passing Moores Run (Fig. 8). Storm speed increases sharply from 4.8 m s^{-1} 40 min before reaching Moores Run to a value of 8.9 m s^{-1} while passing over Moores Run. Storm speed is influenced by growth and collapse of storm cells. Storm direction is generally toward the northeast, with a median value of 67° counterclockwise from the east.

Collapse of the Moores Run storm can best be seen through time series of maximum reflectivity and echo-top height (Fig. 9). The maximum reflectivity peaks at a value of 64.5 dBZ 11 min before passing over Moores Run, then decreases to a value of 54.5 dBZ 1 h after passing Moores Run. The echo-top height shows a similar pattern, reaching a maximum value of 9.75 km 21 min before passing over Moores Run, then decreasing to a value of 5.75 km 1 h after passing Moores Run. The height of the maximum reflectivity reaches its largest value of 6.5 km 16 min before reaching Moores Run. The decrease in area, decrease in maximum reflectivity, and decrease in echo-top height indicate the collapse of the storm cell as it passes Moores Run.

c. *1 June 2006 storm*

The 1 June 2006 storm produced the second-largest discharge (115 m^3 s^{-1}) in Moores Run over the study period (Table 2). The flood peak occurred in the evening at 1918 EST (0018 UTC 2 June 2006). The maximum 15-min rain rate is 66 mm h^{-1}, which ranks as the eleventh largest in 15-min rain rate among the 32 flood events. The storm total rainfall accumulation of 59 mm is not exceptional, compared with the 31 other flood events. The storm is most exceptional at the 30-min time interval, with a rain rate of 61 mm h^{-1} (Fig. 10).

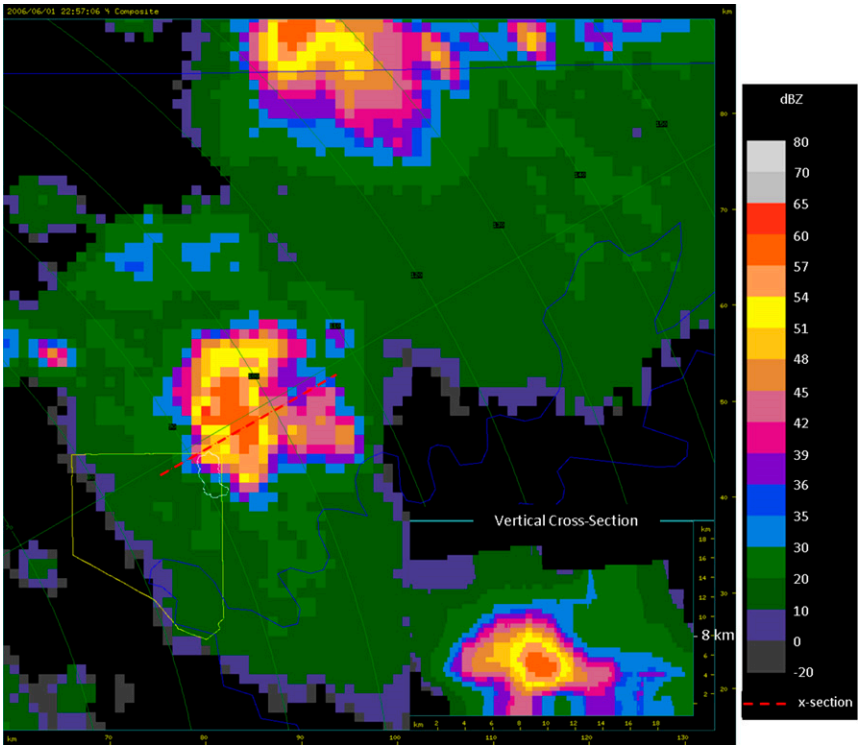

FIG. 11. As in Fig. 5, but for the 1 Jun 2006 storm at 2257 UTC 1 Jun 2006.

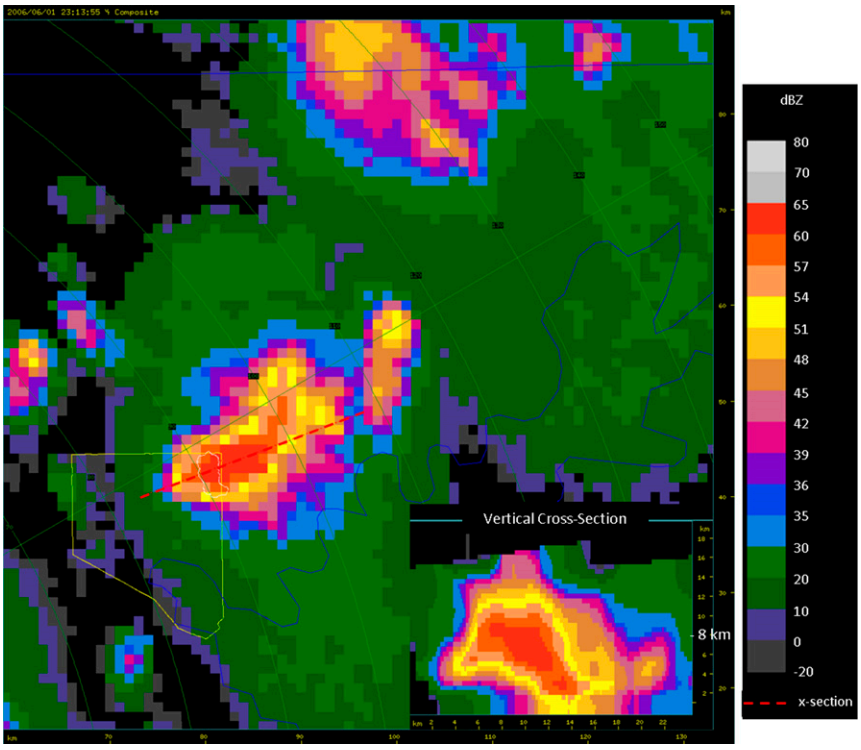

FIG. 12. As in Fig. 11, but for the 1 Jun 2006 storm at 2313 UTC 1 Jun 2006.

The 1 June 2006 flash flood was caused by a system of slow-moving thunderstorms that did not exhibit any linear organization prior to or during the period of heavy rainfall over Moores Run. An intense storm cell, with reflectivity up to 65 dBZ, formed north of Baltimore and moved slowly southeast to Moores Run. The storm cell remained over Moores Run for nearly an hour, merging with storm cells that moved in from the west, and then eventually organized into a linear storm and moved eastward away from Moores Run (Figs. 11–14).

The storm area generally increases as the storm passes Moores Run, from a value of 114 km^2 1 h before passing Moores Run to a value of 934 km^2 1 h after passing Moores Run (Fig. 15). This increase in area represents growth of the newly formed complex storm track and creation of new (simple track) storm cells. There is a small decrease in storm area from 838 to 616 km^2 as the storm passes over Moores Run.

The anomalous behavior observed in the movement of the 1 June 2006 storm is reflected in the time series of storm speed and direction (Fig. 15). The storm moves in an unusual direction before the flood, between 124° and 167° from east (from northwest to west). As the storm reaches Moores Run, it changes direction and begins to move northeast at 86°–98°. This change in direction marks the storm movement over Moores Run and the eventual evolution into a linear storm structure. The storm speed remains low as the storm passes over Moores Run, with a mean velocity of 3.9 m s^{-1}. As the storm moves past Moores Run and develops a linear storm structure, the velocity increases to an average of 8.3 m s^{-1}.

The echo-top height decreases for the 1 June 2006 storm, from 16.25 km 13 min before it passes over Moores Run to 9.75 km 4 min after passing Moores Run (Fig. 16). The maximum reflectivity does not show a clear decrease, and is quite variable between 57 and 66 dBZ within 1 h of the flood-producing rainfall hitting Moores Run. The height of the maximum reflectivity remains near 4 km as the storm passes Moores Run. Time series of maximum reflectivity and maximum reflectivity height indicate that the storm is a low-echo centroid (LEC) storm, with extreme reflectivity at low levels driving the rainfall as the storm hit Moores Run. These LEC storms have been found to cause flooding in other urban areas, such as Fort Collins, Colorado (Petersen et al. 1999).

d. Composite storm characteristics

Storm patterns from the 13 June 2003 and 1 June 2006 storms were used as a basis to analyze the 32-storm

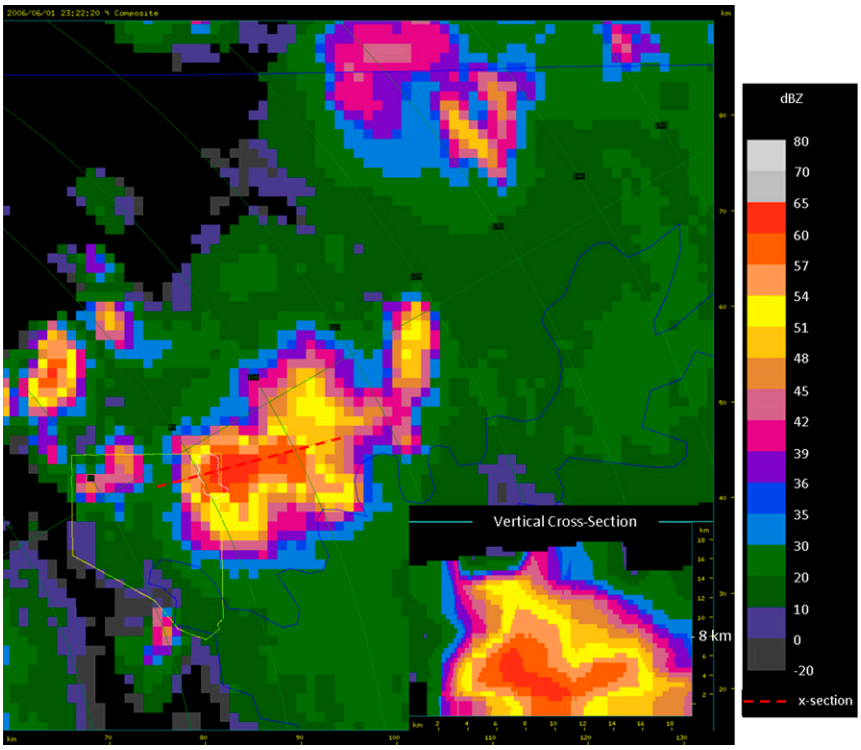

FIG. 13. As in Fig. 11, but for the 1 Jun 2006 storm at 2322 UTC 1 Jun 2006.

sample. We examine the roles of collapsing storm cells, slow storm motion, LEC, and linear organization in the structure of flash flood–producing storms.

Storm organization is roughly similar to the 13 June 2003 and 1 June 2006 storms, with 50% of storms being organized in a linear manner and 50% of storms not having linear organization at the time they hit Moores Run. Storms with linear organization include squall lines and quasi-linear storms. Storms without linear organization tend to be scattered, unorganized storms. The distinction between linear storms and storms without linear organization was made by tracking all storms at a lower reflectivity threshold of 42 dBZ to include multiple nearby storms cells within the same tracks. Then storms with large areas (over 500 km^2) and large aspect ratios (major ellipse axis/minor ellipse axis over 3) were identified as linear. Storms that met only one criterion were categorized via observation of radar data.

Like the 13 June 2003 storm system, storms tend to move from east to northeast near Moores Run (Fig. 17). Average storm direction, at the time the storms pass Moores Run, is most commonly 0°–30°, and 28 storms are between 0° and 120°. Storms tend to exhibit north–south orientation, with 17 storms oriented within 30° of north–south.

Flood-producing storms tend to be elliptical at the time they pass Moores Run, with a median aspect ratio of 2.6 (Fig. 18). The median complex track area, at the time the storms pass Moores Run, is 389 km^2, less than the area for the 13 June 2003 storm or the 1 June 2006 storm. Only eight storms had areas that exceeded 1000 km^2; the 23 July 2008 and 29 June 2012 storms were large, with areas of 2780 and 3120 km^2, respectively. They ranked as the twenty-fourth- and eleventh-largest peak discharge events.

Storm speeds when passing Moores Run range widely, with 0.10 and 0.90 quantiles at 3.8–18.1 m s^{-1} and a median value of 8.9 m s^{-1} (Fig. 18). Storm speed data suggest that slow storms, like the 1 June 2006 storm, do account for some portion of flash flood events. Maximum reflectivity values indicate heavy to extremely heavy rainfall with values ranging from 52.2 to 61.3 dBZ for the 0.10–0.90 quantiles. The height of these maximum reflectivities varies considerably by storm, ranging from 1.5 to 6.0 km. Echo-top height displays similar variation, with values ranging from 4.6 to 10.9 km. The low maximum reflectivity heights and echo-top heights indicate that LEC storms do produce flash floods in Moores Run.

Storms that cause flash flooding in Moores Run have storm centroids that typically pass through Moores Run

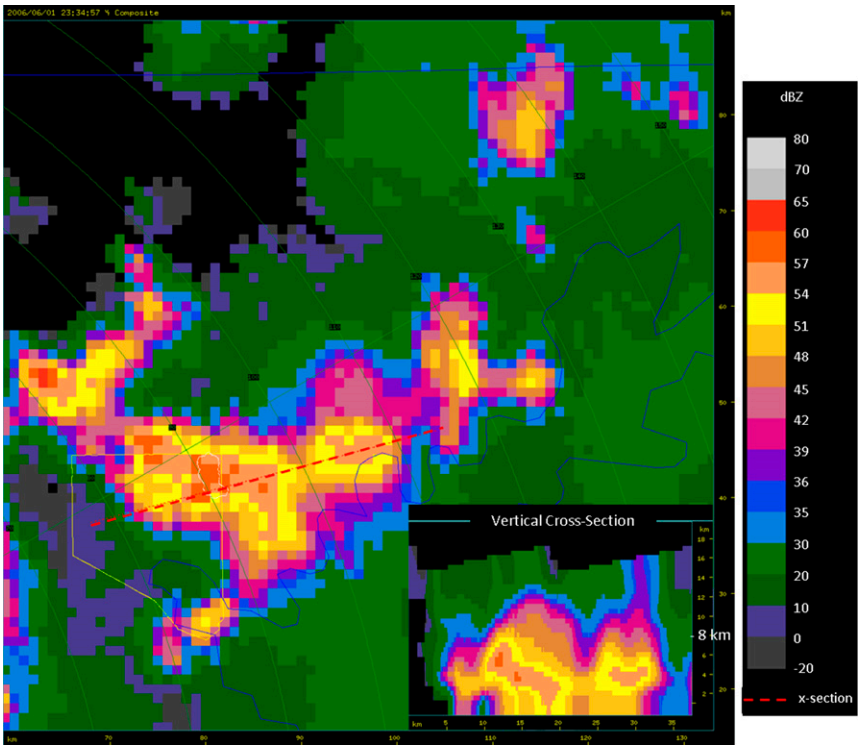

FIG. 14. As in Fig. 11, but for the 1 Jun 2006 storm at 2334 UTC 1 Jun 2006.

(Fig. 19). The density of complex tracks, calculated from the location of the reflectivity centroid for all simple tracks contained within flood-producing complex tracks, is greatest over and to the northeast of Moores Run. The spatial pattern is similar to that for storm-averaged rainfall (Fig. 2). These figures suggest that a consistent characteristic of flash flood–producing storms in Moores Run is that their centroids predominantly pass directly over Moores Run. The increased density of tracks over and downwind of Baltimore also suggests that intense, flash flood–producing storms do not split around Baltimore. Observation of storm tracks with radar reflectivity data also did not provide evidence of storm splitting for the 32 storm events. Storms-producing flash floods in Baltimore are not associated with storm splitting, as has

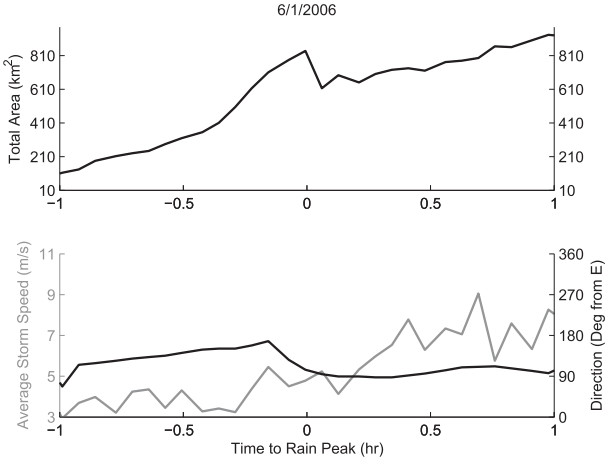

FIG. 15. As in Fig. 8, but for the 1 Jun 2006 storm.

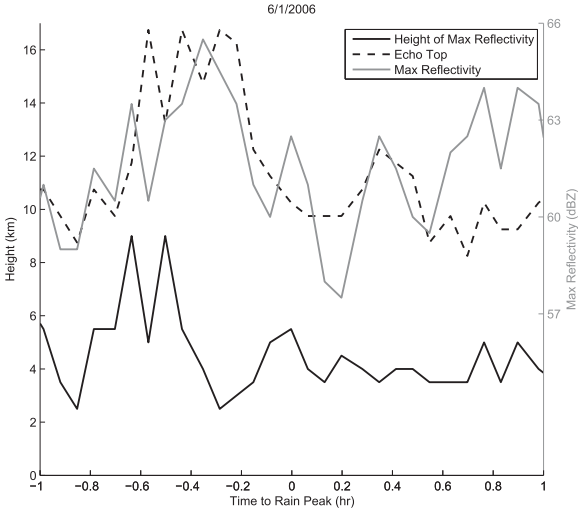

FIG. 16. As in Fig. 9, but for the 1 Jun 2006 storm.

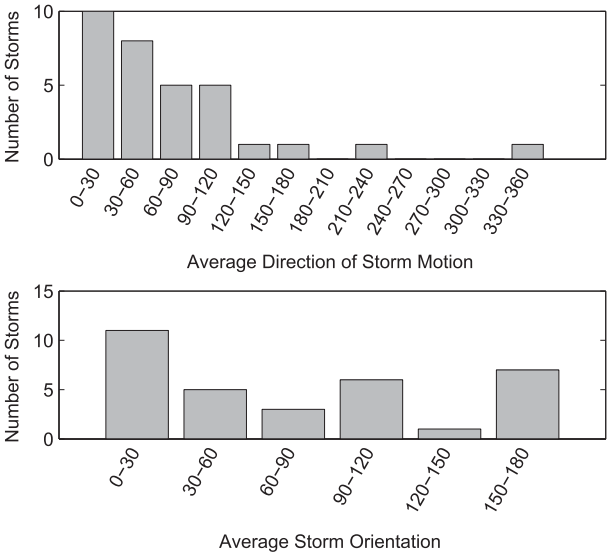

FIG. 17. (top) Average direction of motion for the largest simple track storm cell of the flood-producing complex track in degrees counterclockwise from east. (bottom) Average orientation of the ellipse major axis for the largest simple track of the complex track in degrees clockwise from north.

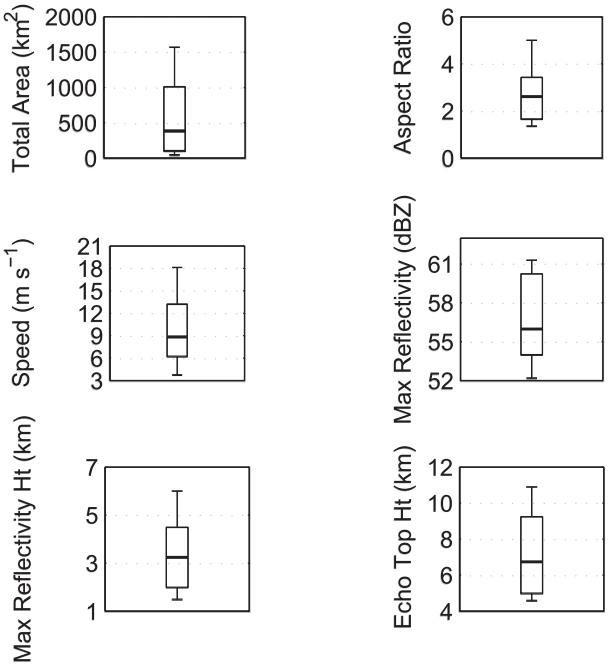

FIG. 18. Box plots of characteristics of flood-producing storms at the time they hit Moores Run (time 0). Boxes represent 25th and 75th quantiles, lines represent medians, and whiskers extend to 10th and 90th quantiles. (top left) Total area of flood-producing complex track, (top right) average aspect ratio (major axis/minor axis lengths) of ellipse for the largest simple track of the flood-producing complex track, (middle left) average speed of the simple tracks included in the flood-producing complex track, (middle right) max reflectivity of the extended simple track, (bottom left) height of max reflectivity of the extended simple track, and (bottom right) echo-top height of extended simple track.

been shown for convective systems in other urban areas (Bornstein and Lin 2000).

Storm-tracking methods developed above were applied to all 32 storm events. To create comparable time series across all storms, the time series for each individual storm were smoothed with a moving average over the period of study. These smoothed time series were normalized by the time series value at time 0. Quantiles for time series values were calculated from these smoothed, normalized data.

Storm size, as represented by the area of the complex track passing over Moores Run, tends to reach a maximum as the storm passes over Moores Run (Fig. 20). The median storm size increases gradually for approximately 15 min, then decreases steadily. There are populations of storms that decay rapidly, as reflected in the 0.25 quantile, and a population of storms that increase in area for approximately 30 min after passing over the basin.

Storm speed generally increases slightly as the storms approach and pass Moores Run, particularly for the top 25th percentile of storm speeds (Fig. 21). This increase in speed may be related to the organization of storm cells into a line as observed in the 1 June 2006 storm. Stronger outflows associated with an organized storm system could be increasing speed.

Measures of storm intensity decrease soon after the storms pass Moores Run, suggesting that many storms are collapsing. Time series of normalized echo-top height (Fig. 22) and normalized maximum reflectivity (Fig. 23) have a similar shape. Both time series feature a maximum value beginning 10–20 min before the storms reach Moores Run and lasting until the storms reach Moores Run. After passing Moores Run, the storms tend to decrease in both echo-top height and reflectivity over a period of 30–45 min. This decreasing pattern is similar to the 13 June 2003 storm cell collapse. Observations of spatial radar reflectivity and vertical reflectivity cross sections for the 32 individual storm events indicated that nearly half the storm events (14) involved storm cell collapse.

Storms were divided into the linearly organized storms and storms without linear organization to see their impacts on storm evolution. Normalized total area time series of storms without linear organization (Fig. 24) closely resemble time series for the entire 32-storm selection (Fig. 20), with a maximum value during times 0–0.5 h and a decrease to 0.76 of their maximum value 1 h after passing Moores Run. Normalized total

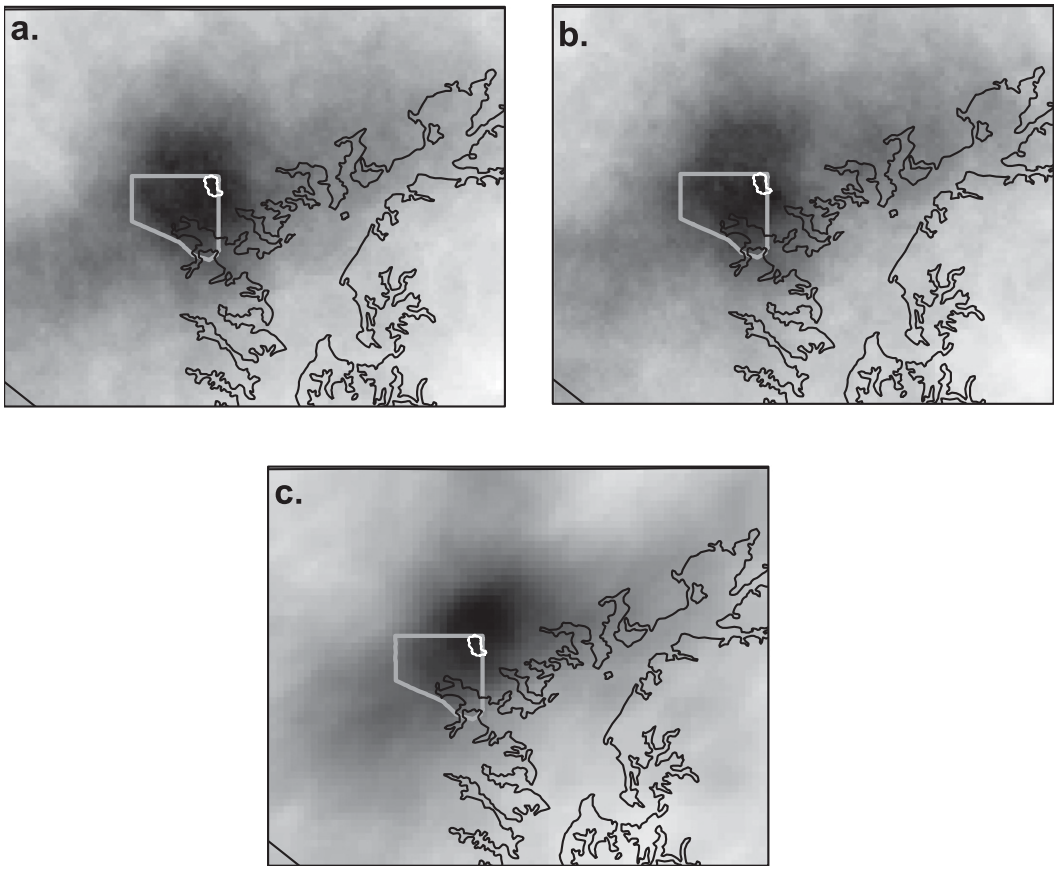

FIG. 19. Density of storm tracks passing through Moores Run for all simple tracks contained in the flood-producing complex tracks for the 32-storm events. Densities are for (a) simple tracks starts, (b) simple tracks ends, and (c) all simple tracks. Darker values represent higher densities. Moores Run is outlined in white and Baltimore is outlined in gray.

area time series for linear storms, however, display a different trend, with maximum values at time 0 and a decrease in total area starting shortly after the storms reach Moores Run.

Convective intensity trends in the 32-storm sample more closely resemble those of linear storms. Both normalized echo-top height (Fig. 25) and normalized maximum reflectivity (Fig. 26) decrease in the 30 min after the storm reaches Moores Run for linearly organized storms. Time series of normalized echo-top height and normalized maximum reflectivity show relatively steady values for storms without linear organization. The normalized echo-top height has a slowly decreasing trend after passing Moores Run for storms without linear organization, while the normalized maximum reflectivity is more varying. These results suggest that the pattern of storm collapse exhibited by the 13 June 2003 storm is more prevalent in linear storms. However, radar observations of storm collapse are divided, with six of the collapsing storms being linearly organized at the time of the flash flood–producing rain and eight storms that do not exhibit linear organization.

4. Summary and conclusions

We characterize flash flood–producing storms in a prototypical urban watershed in the mid-Atlantic United States using Lagrangian analyses. The 13 June 2003 and 1 June 2006 storms were used as storm patterns in order to generalize the structure and evolution of storms that produce flash flooding in Moores Run. The 13 June 2003 flood was produced by a thunderstorm system with linear organization and a storm cell that collapsed over Moores Run, causing extreme 15-min rainfall rates. The 1 June 2006 flood was produced by a thunderstorm system with anomalous storm motion and an absence of linear organization through its life cycle. The storm exhibited an LEC. Our methods were extended to a sample of 32 storms that produced the

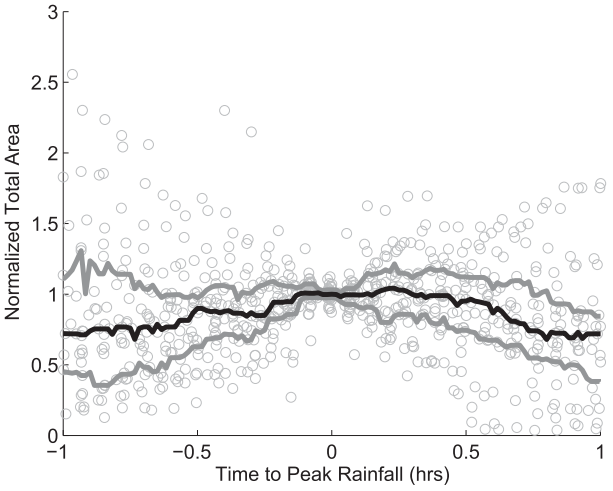

FIG. 20. Total area of complex tracks for the 32 storm events normalized to the average value of the three readings closest to the time the storm hit Moores Run. The black line represents the median value of the 32 storm events and the gray lines represent the 25th and 75th percentiles. Gray circles represent readings for individual storm events.

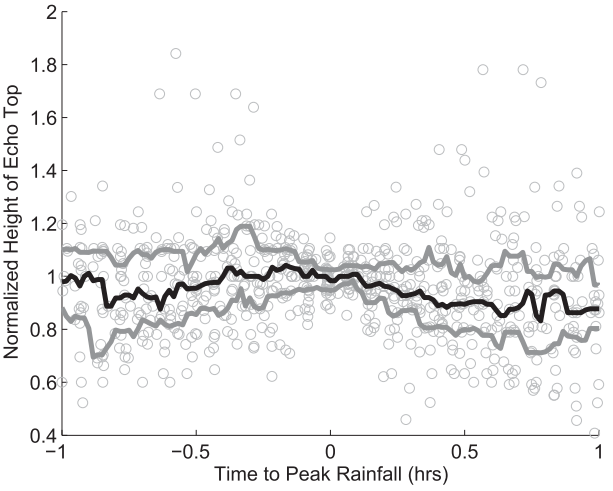

FIG. 22. Height of echo top for extended simple tracks for the 32 storm events normalized to the average value of the three readings closest to the time the storm hit Moores Run. The black line represents the median value of the 32 storm events and the gray lines represent the 25th and 75th percentiles. Gray circles represent readings for individual storm events.

largest flood peaks in Moores Run during the period from January 2000 to May 2014. The main conclusions are summarized below.

1) Flash flooding in Moores Run is often associated with collapsing thunderstorm cells. The time evolution of echo-top height and maximum reflectivity indicate that 14 of the 32 events exhibited storm cell collapse. The 13 June 2003 storm collapsed over Moores Run and produced the flood of record for the watershed. It appears that storm cell collapse is an important and recurring mechanism for generating the intense short-term rain rates that drive flash flooding in small urban watersheds.

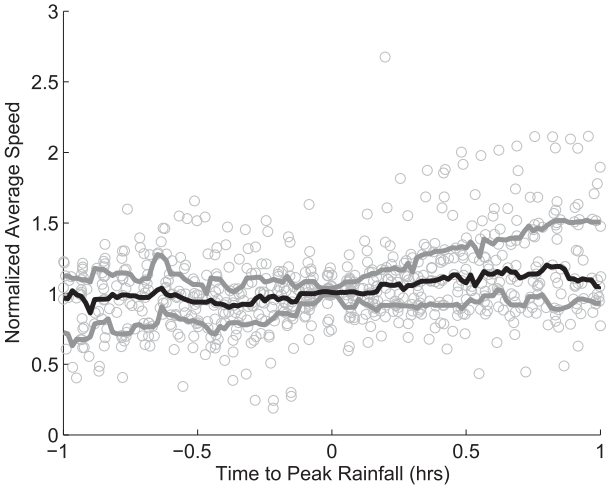

FIG. 21. Average speed of simple tracks included in flood-producing complex tracks for the 32 storm events normalized to the average value of the three readings closest to the time the storm hit Moores Run. The black line represents the median value of the 32 storm events and the gray lines represent the 25th and 75th percentiles. Gray circles represent readings for individual storm events.

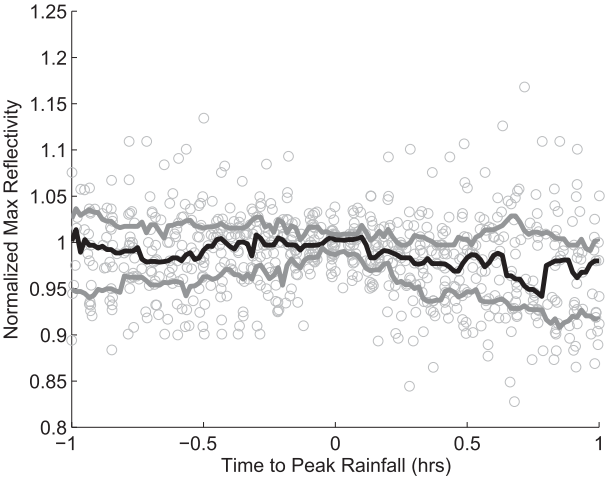

FIG. 23. Max reflectivity for extended simple tracks for the 32 storm events normalized to the average value of the three readings closest to the time the storm hit Moores Run. The black line represents the median value of the 32 storm events and the gray lines represent the 25th and 75th percentiles. Gray circles represent readings for individual storm events.

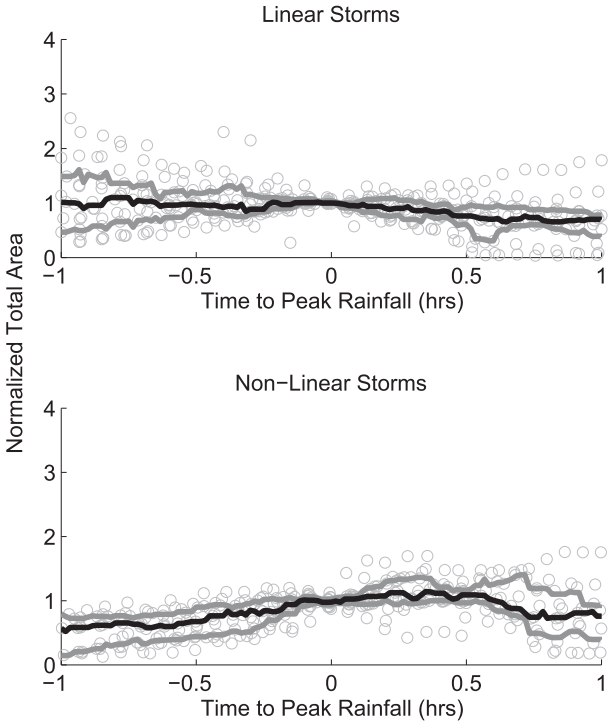

FIG. 24. Total area of complex tracks for (top) the 16 linearly organized storm events and (bottom) the 16 storm events without linear organization normalized to the average value of the three readings closest to the time the storm hit Moores Run. The black line represents the median value of the 32 storm events and the gray lines represent the 25th and 75th percentiles. Gray circles represent readings for individual storm events.

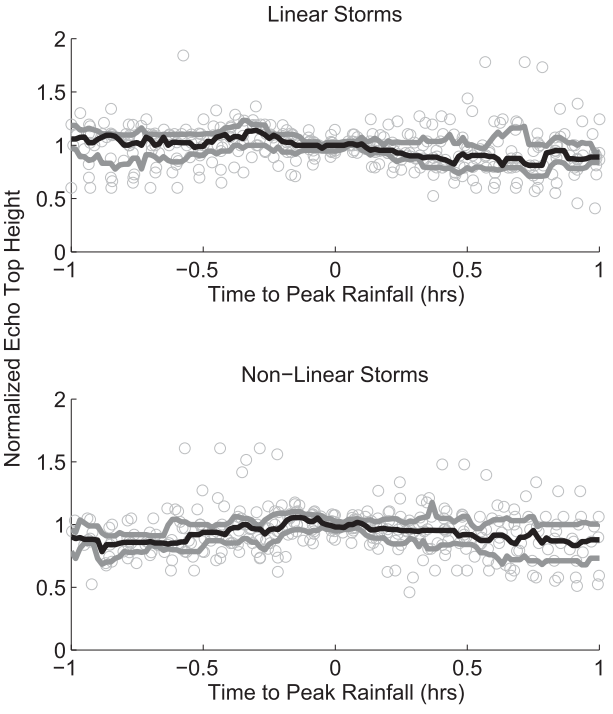

FIG. 25. As in Fig. 24, but for echo-top height for extended simple tracks.

2) Flash flood–producing rainfall in Moores Run is spatially and temporally concentrated. The maximum storm-averaged rainfall contour (65 mm) for the 32 storms is centered over the Moores Run watershed. Average rainfall accumulations decrease rapidly upwind of the watershed (1.8 mm km^{-1}) and decrease less rapidly downwind of the watershed (0.6 mm km^{-1}). This difference can be attributed to urban modification of rainfall. The maximum 15-min rainfall accumulation accounts for 21% of the storm total rainfall on average. There are pronounced diurnal and seasonal impacts on flash flood occurrence, with floods predominantly occurring during the evening and warm season.
3) Storm evolution sampled from 32 events is dominated by motion from southwest to northeast, with 18 of the storms moving between 0° and 60° (east and north-northeast). Storms are split evenly between those with linear organization and those without linear organization. Storm structure is often characterized by a north–south orientation (especially for storms with linear organization), with 17 storms oriented within 30° of north–south. Storm speed is highly variable for the 32-event sample, with 4.8 m s^{-1} for the 1 June 2006 storm on the low end

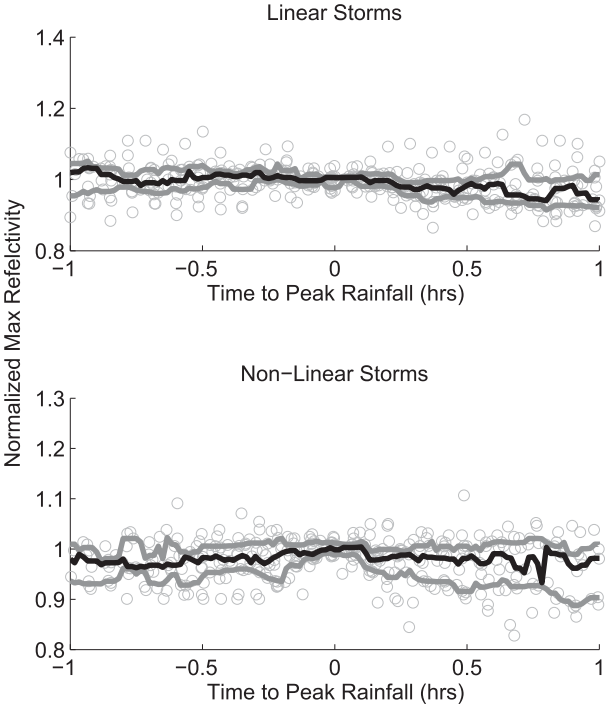

FIG. 26. As in Fig. 24, but for max reflectivity for extended simple tracks.

and 8.9 m s^{-1} for the 13 June 2003 storm close to the median value; peak values of storm speed exceed 20 m s^{-1}. Storm size ranges from 19 to 3120 km^2. Both the 13 June 2003 storm and 1 June 2006 storm show steady increases in storm size leading up to the period of peak rainfall and flooding.

4) A number of typical flash flood–producing storm characteristics are identified; these include occurrence of evening storms in the warm season, northeast storm motion, and north–south storm orientation. Storm reflectivities were greater than 52 dBZ, and storm heights varied greatly between storm events.
5) Storm tracks for flash flood–producing storms do not generally split around Baltimore. The density of storm tracks is concentrated in a southwest-to-northeast-oriented ellipse centered on the Moores Run watershed. The distribution of storm initiation locations, which include the locations of storm splits, exhibits a circular distribution with a peak in central Baltimore.
6) Storm organization is linked with evolution of the storm events. Linearly organized storms exhibited a slowly decreasing trend in total area after passing Moores Run, while storms without linear organization stayed at a maximum area for 30 min after passing Moores Run. Storm cell collapse was more evident for linear storms than for storms without linear organization.

Acknowledgments. The authors would like to acknowledge support for this research from the National Science Foundation (Grants EEC-0540832, CBET-1058027, CBET-1444758, and AGS-1522492) and the NOAA Cooperative Institute for Climate Science.

REFERENCES

Ashley, S. T., and W. S. Ashley, 2008: Flood fatalities in the United States. *J. Appl. Meteor. Climatol.*, **47**, 805–818, doi:10.1175/2007JAMC1611.1.

Austin, G., and A. Bellon, 1982: Very-short-range forecasting of precipitation by the objective extrapolation of radar and satellite data. *Nowcasting*, K. A. Browning, Ed., Academic Press, 177–190.

Berne, A., G. Delrieu, J. D. Creutin, and C. Obled, 2004: Temporal and spatial resolution of rainfall measurements required for urban hydrology. *J. Hydrol.*, **299**, 166–179, doi:10.1016/S0022-1694(04)00363-4.

Bhaskar, A., and C. Welty, 2012: Water balances along an urban-to-rural gradient of metropolitan Baltimore. *Environ. Eng. Geosci.*, **18**, 37–50, doi:10.2113/gseegeosci.18.1.37.

Booth, D. B., 1990: Stream-channel incision following drainage basin urbanization. *J. Amer. Water Resour. Assoc.*, **26**, 407–417, doi:10.1111/j.1752-1688.1990.tb01380.x.

Bornstein, R., and Q. Lin, 2000: Urban heat islands and summertime convective thunderstorms in Atlanta: Three case studies. *Atmos. Environ.*, **34**, 507–516, doi:10.1016/S1352-2310(99)00374-X.

Dixon, M., and G. Wiener, 1993: TITAN: Thunderstorm Identification, Tracking, Analysis, and Nowcasting—A radar-based methodology. *J. Atmos. Oceanic Technol.*, **10**, 785–797, doi:10.1175/1520-0426(1993)010<0785:TTITAA>2.0.CO;2.

Doswell, C., H. Brooks, and R. Maddox, 1996: Flash flood forecasting: An ingredients-based methodology. *Wea. Forecasting*, **11**, 560–581, doi:10.1175/1520-0434(1996)011<0560:FFFAIB>2.0.CO;2.

Elsner, J., W. Drag, and J. Last, 1989: Synoptic weather patterns associated with the Milwaukee, Wisconsin flash flood of 6 August 1986. *Wea. Forecasting*, **4**, 537–554, doi:10.1175/1520-0434(1989)004<0537:SWPAWT>2.0.CO;2.

Javier, J. R. N., J. A. Smith, J. England, M. L. Baeck, M. Steiner, and A. A. Ntelekos, 2007: Climatology of extreme rainfall and flooding from orographic thunderstorm systems in the upper Arkansas River basin. *Water Resour. Res.*, **43**, W10410, doi:10.1029/2006WR005093.

Jessup, S., and S. Colucci, 2012: Organization of flash-flood-producing precipitation in the northeast United States. *Wea. Forecasting*, **27**, 345–361, doi:10.1175/WAF-D-11-00026.1.

Krajewski, W. F., and Coauthors, 2011: Towards better utilization of NEXRAD data in hydrology: An overview of Hydro-NEXRAD. *J. Hydroinform.*, **13**, 255–266, doi:10.2166/hydro.2010.056.

Lakshmanan, V., and T. Smith, 2010: An objective method of evaluating and devising storm-tracking algorithms. *Wea. Forecasting*, **25**, 701–709, doi:10.1175/2009WAF2222330.1.

Li, D., E. Bou-Zeid, M. Baeck, S. Jessup, and J. Smith, 2013: Modeling land surface processes and heavy rainfall in urban environments: Sensitivity to urban surface representations. *J. Hydrometeor.*, **14**, 1098–1118, doi:10.1175/JHM-D-12-0154.1.

Maddox, R. A., C. F. Chappell, and L. R. Hoxit, 1979: Synoptic and meso-α scale aspects of flash flood events. *Bull. Amer. Meteor. Soc.*, **60**, 115–123, doi:10.1175/1520-0477-60.2.115.

Meierdiercks, K. L., J. A. Smith, M. L. Baeck, and A. J. Miller, 2010: Heterogeneity of hydrologic response in urban watersheds. *J. Amer. Water Resour. Assoc.*, **46**, 1221–1237, doi:10.1111/j.1752-1688.2010.00487.x.

Mooney, L., 1983: Applications and implications of fatality statistics to the flash flood problem. Preprints, *Fifth Conf. on Hydrometeorology*, Tulsa, OK, Amer. Meteor. Soc., 127–129.

Morin, E., Y. Enzel, U. Shamir, and R. Garti, 2001: The characteristic time scale for basin hydrological response using radar data. *J. Hydrol.*, **252**, 85–99, doi:10.1016/S0022-1694(01)00451-6.

Nelson, P. A., J. A. Smith, and A. J. Miller, 2006: Evolution of channel morphology and hydrologic response in an urbanizing drainage basin. *Earth Surf. Processes Landforms*, **31**, 1063–1079, doi:10.1002/esp.1308.

Niyogi, D., P. Pyle, M. Lei, S. P. Arya, C. M. Kishtawal, M. Sheperd, F. Chen, and B. Wolfe, 2011: Urban modification of thunderstorms: An observational storm climatology and model case study for the Indianapolis urban region. *J. Appl. Meteor. Climatol.*, **50**, 1129–1144, doi:10.1175/2010JAMC1836.1.

Ntelekos, A. A., J. A. Smith, and W. F. Krajewski, 2007: Climatological analyses of thunderstorms and flash floods in the Baltimore metropolitan region. *J. Hydrometeor.*, **8**, 88–101, doi:10.1175/JHM558.1.

——, ——, M. L. Baeck, W. F. Krajewski, A. J. Miller, and R. Goska, 2008: Extreme hydrometeorological events and the urban environment: Dissecting the 7 July 2004 thunderstorm over the Baltimore, MD, metropolitan region. *Water Resour. Res.*, **44**, W08446, doi:10.1029/2007WR006346.

Ogden, F. L., H. O. Sharif, S. U. S. Senarath, J. A. Smith, M. L. Baeck, and J. R. Richardson, 2000: Hydrologic analysis of the Fort Collins, Colorado, flash flood of 1997. *J. Hydrol.*, **228**, 82–100, doi:10.1016/S0022-1694(00)00146-3.

Paul, M. J., and J. L. Meyer, 2001: Streams in the urban landscape. *Annu. Rev. Ecol. Syst.*, **32**, 333–365, doi:10.1146/annurev.ecolsys.32.081501.114040.

Peleg, N., and E. Morin, 2012: Convective rain cells: Radar-derived spatiotemporal characteristics and synoptic patterns over the eastern Mediterranean. *J. Geophys. Res.*, **117**, D15116, doi:10.1029/2011JD017353.

Petersen, W. A., and Coauthors, 1999: Mesoscale and radar observations of the Fort Collins flash flood of 28 July 1997. *Bull. Amer. Meteor. Soc.*, **80**, 191–216, doi:10.1175/1520-0477(1999)080<0191:MAROOT>2.0.CO;2.

Pontrelli, M. D., G. Bryan, and J. M. Fritsch, 1999: The Madison County flash flood of 27 June 1995. *Wea. Forecasting*, **14**, 384–404, doi:10.1175/1520-0434(1999)014<0384:TMCVFF>2.0.CO;2.

Ryu, Y. H., J. A. Smth, M. L. Baeck, and E. Bou-Zeid, 2016: The influence of land-surface heterogeneities on heavy convective rainfall in the Baltimore–Washington metropolitan area. *Mon. Wea. Rev.*, **144**, 553–573, doi:10.1175/MWR-D-15-0192.1.

Schumacher, R. S., and R. H. Johnson, 2005: Organization and environmental properties of extreme-rain-producing mesoscale convective systems. *Mon. Wea. Rev.*, **133**, 961–976, doi:10.1175/MWR2899.1.

——, and ——, 2008: Mesoscale processes contributing to extreme rainfall in a midlatitude warm-season flash flood. *Mon. Wea. Rev.*, **136**, 3964–3986, doi:10.1175/2008MWR2471.1.

Schwartz, B., C. Chappell, W. Togstad, and X. Zhong, 1990: The Minneapolis flash flood: Meteorological analysis and operational response. *Wea. Forecasting*, **5**, 3–21, doi:10.1175/1520-0434(1990)005,0003:TMFFMA.2.0.CO;2.

Schwartz, S., and B. Smith, 2014: Slowflow fingerprints of urban hydrology. *J. Hydrol.*, **515**, 116–128, doi:10.1016/j.jhydrol.2014.04.019.

Shepherd, J. M., 2005: A review of the current investigations of urban-induced rainfall and recommendations for the future. *Earth Interact.*, **9**, doi:10.1175/EI156.1.

Smith, B. K., and J. A. Smith, 2015: The flashiest watersheds in the contiguous. *J. Hydrometeor.*, **16**, 2365–2381, doi:10.1175/JHM-D-14-0217.1.

——, ——, M. L. Baeck, G. Villarini, and D. B. Wright, 2013: Spectrum of storm event hydrologic response in urban watersheds. *Water Resour. Res.*, **49**, 2649–2663, doi:10.1002/wrcr.20223.

——, ——, ——, and A. J. Miller, 2015: Exploring storage and runoff generation processes for urban flooding through a physically based watershed model. *Water Resour. Res.*, **51**, 1552–1569, doi:10.1002/2014WR016085.

Smith, J. A., A. J. Miller, M. L. Baeck, P. A. Nelson, G. T. Fisher, and K. L. Meierdiercks, 2005: Extraordinary flood response of a small urban watershed to short duration convective rainfall. *J. Hydrometeor.*, **6**, 599–617, doi:10.1175/JHM426.1.

——, M. L. Baeck, G. Villarini, C. Welty, A. J. Miller, and W. F. Krajewski, 2012: Analysis of a long-term, high-resolution radar rainfall data set for the Baltimore metropolitan area. *Water Resour. Res.*, **48**, W04504, doi:10.1029/2011WR010641.

Tapia, A., J. Smith, and M. Dixon, 1998: Estimation of convective rainfall from lightning observations. *J. Appl. Meteor.*, **37**, 1497–1509, doi:10.1175/1520-0450(1998)037<1497:EOCRFL>2.0.CO;2.

Thorndahl, S., J. A. Smith, M. Baeck, and W. Krajewski, 2014: Analyses of the spatial and temporal structures of heavy rainfall from a catalogue of high-resolution radar rainfall fields. *Atmos. Res.*, **144**, 111–125, doi:10.1016/j.atmosres.2014.03.013.

Wright, D. B., J. A. Smith, G. Villarini, and M. L. Baeck, 2012: Hydroclimatology of flash flooding in Atlanta. *Water Resour. Res.*, **48**, W04524, doi:10.1029/2011WR011371.

Yang, L., J. A. Smith, D. B. Wright, M. L. Baeck, and G. Villarini, 2013: Urbanization and climate change: An examination of nonstationarities in urban flooding. *J. Hydrometeor.*, **14**, 1791–1809, doi:10.1175/JHM-D-12-095.1.

Yeung, J., J. Smith, M. Baeck, and G. Villarini, 2015: Lagrangian analyses of rainfall structure and evolution for organized thunderstorm systems in the urban corridor of the northeastern United States. *J. Hydrometeor.*, **16**, 1575–1595, doi:10.1175/JHM-D-14-0095.1.